

# A comparative study of polaronic transport in paramagnetic state of bulk and nanocrystalline $\text{La}_{0.46}\text{Ca}_{0.54}\text{MnO}_3$ compound

Kalipada Das

Citation: *Journal of Applied Physics* **124**, 125104 (2018); doi: 10.1063/1.5042338

View online: <https://doi.org/10.1063/1.5042338>

View Table of Contents: <http://aip.scitation.org/toc/jap/124/12>

Published by the *American Institute of Physics*

---

---

**HIDEN**  
ANALYTICAL

## Instruments for Advanced Science

Contact Hiden Analytical for further details:

**W** [www.HidenAnalytical.com](http://www.HidenAnalytical.com)

**E** [info@hiden.co.uk](mailto:info@hiden.co.uk)

**CLICK TO VIEW** our product catalogue



### Gas Analysis

- ▶ dynamic measurement of reaction gas streams
- ▶ catalysis and thermal analysis
- ▶ molecular beam studies
- ▶ dissolved species probes
- ▶ fermentation, environmental and ecological studies



### Surface Science

- ▶ UHV TPD
- ▶ SIMS
- ▶ end point detection in ion beam etch
- ▶ elemental imaging - surface mapping



### Plasma Diagnostics

- ▶ plasma source characterization
- ▶ etch and deposition process reaction kinetic studies
- ▶ analysis of neutral and radical species



### Vacuum Analysis

- ▶ partial pressure measurement and control of process gases
- ▶ reactive sputter process control
- ▶ vacuum diagnostics
- ▶ vacuum coating process monitoring

# A comparative study of polaronic transport in paramagnetic state of bulk and nanocrystalline $\text{La}_{0.46}\text{Ca}_{0.54}\text{MnO}_3$ compound

Kalipada Das<sup>a)</sup>*Department of Physics, Seth Anandram Jaipuria College, 10 Raja Naba Krishna Street, Kolkata 700005, India*

(Received 31 May 2018; accepted 9 September 2018; published online 27 September 2018)

In this present study, electronic transport and magneto-transport properties of bulk and nanocrystalline  $\text{La}_{0.46}\text{Ca}_{0.54}\text{MnO}_3$  compound are reported. The activation energies required for polaron transport in the paramagnetic state for different average grain size particles were estimated from the resistivity as a function of temperature data. It is found that there is a strong dependency of the activation energy in paramagnetic state with the reduction of the grain sizes and charge ordering. With decreasing particle sizes, activation energy enhances and it modifies with the application of external magnetic field. However, a different nature was found for the 15 and 21 nm particle size samples. The activation energy for the 21 nm particle size sample is smaller compared to 15 nm. Such behavior may be associated with the more disorder and spin-pinning effect in the lowest particle size sample. The variation of activation energy and the crystallographic unit cell volume with the reduction of particle size is addressed. *Published by AIP Publishing.* <https://doi.org/10.1063/1.5042338>

## I. INTRODUCTION

In strongly correlated electronic systems, the magnetic and magneto-transport properties were extensively studied during the previous few decades.<sup>1–3</sup> The doped perovskite manganite having the general formula  $\text{RE}_{1-x}\text{B}_x\text{MnO}_3$  where “RE” is rare-earth and B is bivalent ions gets immense attraction due to the strongly correlated nature of their transport and magnetic properties.<sup>4–19</sup> Additionally, the observations of colossal magnetoresistance (CMR) effect, large magnetocaloric effect (MCE), phase-separation, etc., in the doped manganite are also very important aspects for the current research.<sup>14–20</sup> Charge-ordering is one of the most well known phenomena in doped perovskite manganite. Charge-ordering generally occurs in nearly half doped manganite compounds. It is the real space ordering of the  $\text{Mn}^{3+}$  and  $\text{Mn}^{4+}$  ions in a crystal. Charge-ordering phenomena in doped perovskite manganite is observed below a temperature which is called charge-ordering transition temperature ( $T_{co}$ ). The charge-ordering transition is occasionally accompanied by an antiferromagnetic transition with lowering the temperature. From the electronic transport properties, the insulating nature (sharp increase of resistivity) was found with lowering the temperature below charge-ordering. In contrast to the bulk counterparts, the physical properties of the doped perovskite manganite, especially charge-ordered materials, were greatly modified in the nano-scale region.<sup>5,6,9,10,20,21</sup> It is reported that with reduction of the particle size, the antiferromagnetic charge-ordered ground state becomes fragile and it transforms into ferromagnetic in nature.<sup>5,20</sup> Recently, Das *et al.* reported the particle size driven enhancement of magnetoresistance at low temperature of several charge-ordered manganite compounds.<sup>20</sup> According to the reported study by Das *et al.*, normalized resistivity with reduction of the average particle size is

reduced in the low temperature region (below  $T_{co}$ ). Moreover, a strong correlation nature with magnetism and magneto-transport (magnetoresistance) was also reported.<sup>20</sup> However, much less effort was paid to study the magneto-transport properties of such compounds in the high temperature region.

Generally, at the high temperature region, the electron transport mechanism is addressed through the adiabatic polaron hopping mechanism associated with particular activation energy. The value of the activation energy strongly depends on the growth of the resistivity with decreasing temperature in the insulating region (paramagnetic). On the other hand, the resistivity at high temperature also depends on the disorder and pinning center, especially for the nano-scale granular systems. From this context, the activation energy should differ in a reduced particle size sample when compared to the bulk counterpart. Additionally, it is also important to mention that since the effect of the different counterparts of resistivity is different depending upon the temperature range, the nature of the activation energy may also be different according to the temperature scale.

In our present study, we have estimated the variation of the activation energy with reduction of the particle size for  $\text{La}_{0.46}\text{Ca}_{0.54}\text{MnO}_3$  compound in the paramagnetic state. Our study interestingly indicates the anomalous magnetoresistive behavior in the presence of 10 kOe external magnetic field. Such nature (positive MR for larger grain size samples) is analyzed considering the predominant magnetic training effect as reported earlier.<sup>21</sup>

At the end of this part, a brief discussion about the  $\text{La}_{0.46}\text{Ca}_{0.54}\text{MnO}_3$  is presented. According to the reported phase diagram for the bulk compound as reported by Cheong and Hwang, this is a charge-ordered antiferromagnetic compound.<sup>1</sup> The charge-ordering transition is  $T = 260$  K, which is followed by an antiferromagnetic transition  $T = 150$  K. Additionally, the pronounced training effect was found in the bulk compound, and it gets reduced with reduction of the particle size.<sup>21</sup> At the low temperature region,

<sup>a)</sup>Electronic mail: kalipadadasphysics@gmail.com

magnetoresistance enhancement appears with reduction of the particle size.<sup>20</sup> Regarding the issue of the training effect observed in this compound, it is worth mentioning that in the case of the 15 nm particle size sample, the charge ordered state was absent.<sup>21</sup> In our previous report, the correlation between the training effect and the charge ordering was addressed for this compound where the training effect was absent in the case of the lowest particle size sample.<sup>21</sup>

## II. SAMPLE PREPARATION, CHARACTERIZATIONS, AND MEASUREMENTS

Nanocrystalline and bulk compound  $\text{La}_{0.46}\text{Ca}_{0.54}\text{MnO}_3$  were prepared by the well known sol-gel route. For systematics in this route, the starting elements pre-heated were  $\text{La}_2\text{O}_3$ ,  $\text{CaCO}_3$ , and  $\text{MnO}_2$ . The constituent elements were dissolved in the millipore water, and gel was prepared as discussed in our previous studies.<sup>20,21</sup> After decomposing the gel at a slightly high temperature (200 °C), black porous powder was formed which was pelletized. The pellet samples were annealed at different temperatures (800–1000 °C) for different time spans (4–10 h) to get different size nanocrystalline samples. However, for preparation of the bulk counterpart, the annealing temperature and annealing time span were large (1300 °C for 36 h). After preparation of the

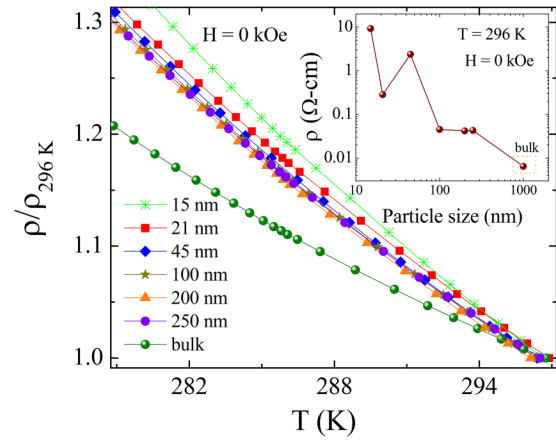


FIG. 1. Normalized resistivity as a function of temperature of  $\text{La}_{0.46}\text{Ca}_{0.54}\text{MnO}_3$  compound at the paramagnetic region in the absence of external magnetic field. The inset indicates the variation of resistivity at  $T = 296 \text{ K}$  as a function of particle sizes.

nanocrystalline and bulk counterpart, the x-ray diffraction study (XRD) was carried out by using a Rigaku-TTRAX-III diffractometer with  $\text{Cu-K}\alpha$  radiation. Transport and magnetotransport measurements were performed by using a home-made insert with a cryogenic magnet system in the four probe method (longitudinal geometry).

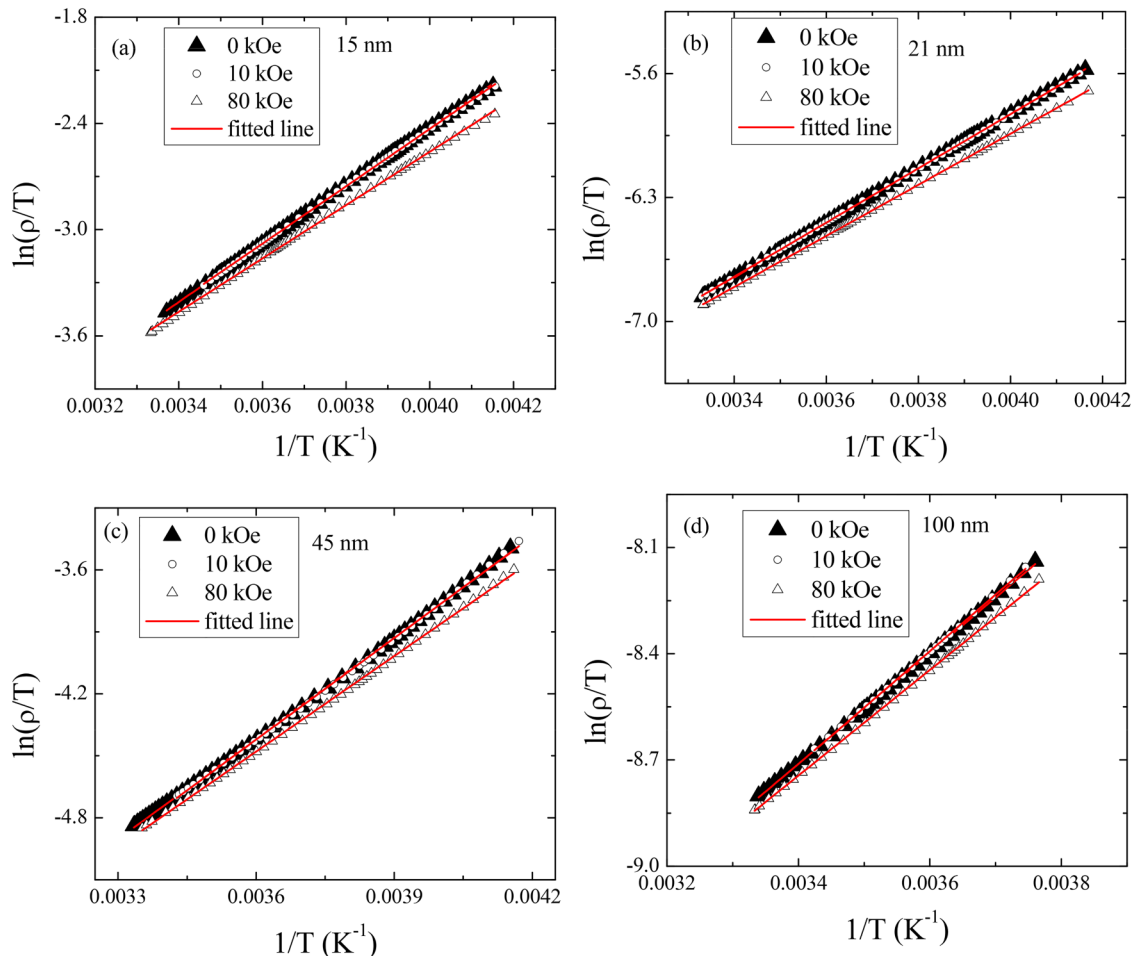


FIG. 2. Variation of  $\ln(\rho/T)$  as a function of  $1/T$  for the nanocrystalline samples 15 nm, 21 nm, 45 nm, and 100 nm in the presence and the absence of magnetic field. Red lines indicate the linear fitting by using Eq. (1).

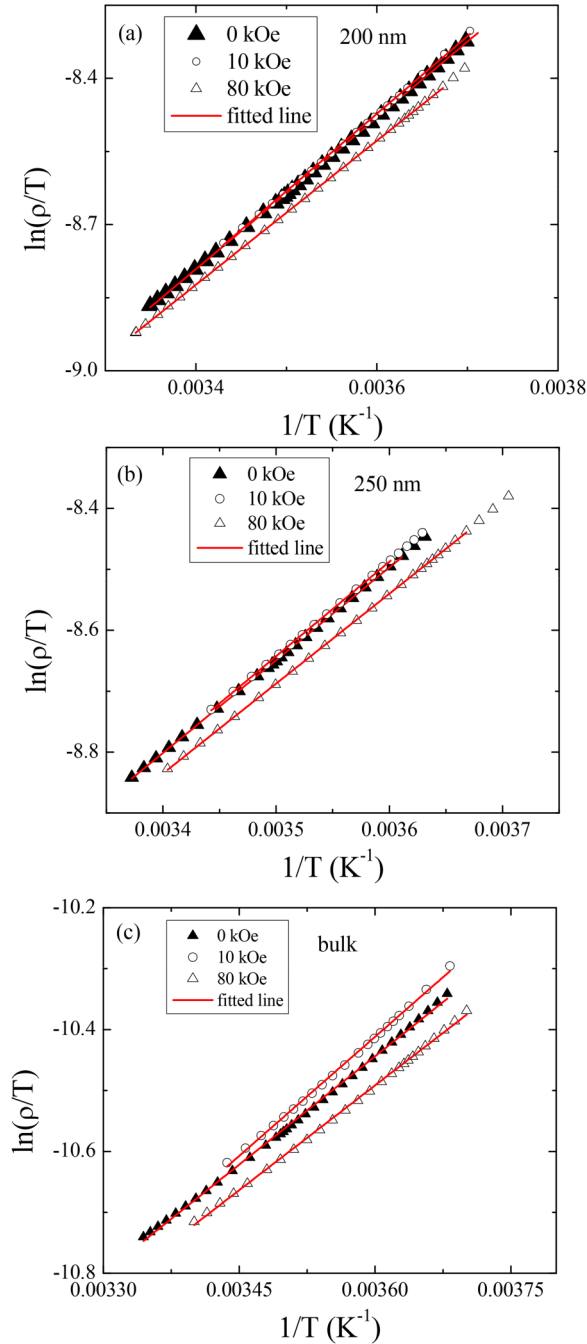


FIG. 3. Variation of  $\ln(\rho/T)$  as a function of  $1/T$  for the nanocrystalline (200 nm and 250 nm) and bulk sample in the presence and the absence of magnetic field. Red lines indicate the linear fitting by using Eq. (1).

### III. RESULTS AND DISCUSSION

X-ray diffraction (XRD) results for the nanocrystalline and bulk sample indicate the single phase nature of the compounds. The XRD patterns for all the samples were fitted by considering the “*pnma*” space group symmetry. Experimentally, XRD patterns along with the Rietveld refinement data of profile fitting is given in Ref. 20. Regarding this context, it should be mentioned that the particle size dependent unit cell volume is calculated, and it is described in the latter part of this paper. The average particle size of nanocrystalline samples was estimated from the x-ray line width broadening as well as from the field emission scanning

TABLE I. Variation of activation energy for nanocrystalline  $\text{La}_{0.46}\text{Ca}_{0.54}\text{MnO}_3$  compound in the absence and presence of different external magnetic fields. Error values are given within the parentheses.

Particle size (nm)	$E_a$ (meV) at 0 kOe	$E_a$ (meV) at 10 kOe	$E_a$ (meV) at 80 kOe
15	141.13 (0.24)	139.32 (0.31)	129.52 (0.42)
21	132.61 (0.08)	131.41 (0.07)	124.01 (0.07)
45	139.75 (0.36)	140.87 (0.46)	132.44 (0.37)
100	134.68 (0.33)	137.17 (0.52)	128.23 (0.26)
200	133.82 (0.32)	136.65 (0.64)	127.19 (0.14)
250	130.89 (0.27)	134.33 (0.34)	126.85 (0.23)
Bulk	101.99 (0.58)	112.14 (0.89)	98.64 (0.57)

electron microscopy study which are given in detail in Refs. 20 and 21. One important point to mention is that in the case of the bulk sample, the average grain size is in the micrometer scale ( $\sim 1000$  nm).

The resistivity as a function of temperature in the absence of any external magnetic field indicates the insulating nature of these compounds.<sup>20,21</sup> Below the charge-ordering transition, resistivity (normalized) sharply increases with decreases of temperature. However, in the low temperature region, the reduction of the resistivity with decreasing particle size was observed.<sup>20</sup> Regarding the discussion about the resistivity of the studied sample, it is important to mention that disorder, pinning center, crystallographic defect, etc., have a substantial impact on the resistivity as well as on its temperature dependence. Existence of the disorder, defect, and spin pinning are the most well known terms in the case of nanomaterials. In this context, due to the larger contribution of the disorder, defect, etc., with reduction of the particle sizes, the resistivity should increase with reduction of the grain sizes. In the case of  $\text{La}_{0.46}\text{Ca}_{0.54}\text{MnO}_3$  compound, the resistivity at the paramagnetic region increases with the reduction of the particle sizes. In the paramagnetic region, the resistivity (normalized) as a function of temperature in the absence of external magnetic field is shown in Fig. 1. The  $\rho(T)$  behavior indicates that the resistivity growth is maximum for the lowest particle size sample ( $\sim 15$  nm). However, it is substantially reduced for the  $\sim 21$  nm sample. The larger values of the resistivity in the case of the lowest particle size samples may be ascribed as the enhanced contribution of disorder, pinning centers, defects, etc., whereas for the 21 nm particle size sample, the above mentioned contributions are reduced compared to the lowest particle size sample. Another point also important to mention here is that the resistivity again increases for the  $\sim 45$  nm particle size and then reduces according to the particle size increment. The enhanced resistivity in the case of the 45 nm particle size sample may be inferred due to the formation of the charge ordered domains within the surface disordered magnetic ground state. The variation of the resistivity in the paramagnetic region ( $T = 296$  K) with the particle size is shown in the inset of Fig. 1.

Very interestingly, it is worth mentioning that in the presence of the lower value of the applied magnetic field, the

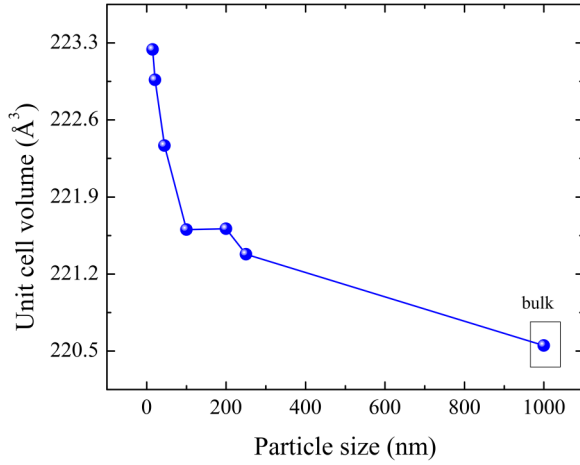


FIG. 4. Variation of the unit cell volume with different particle sizes of  $\text{La}_{0.46}\text{Ca}_{0.54}\text{MnO}_3$  compound.

resistivity increases for the phase separated nanoparticles and bulk counterpart. Such an increasing nature may be explained by considering the magnetic training effect in such phase separated compounds as reported earlier.<sup>21</sup> However, due to the large applied magnetic field, resistivity reduces for all the samples as usual in nature for the phase separated compounds.

The resistivity variation with the temperature at the paramagnetic region in strongly correlated manganite systems is well documented by considering the small polaron hopping mechanism.<sup>22</sup> According to this model, the general expression for the resistivity variation with temperature [ $\rho(T)$ ] is given below by the equation

$$\rho(T) = \rho_0 T \exp\left(\frac{E_a}{K_B T}\right). \quad (1)$$

Here,  $\rho_0$  is the residual resistivity and  $E_a$  is the activation energy ( $K_B$  is the Boltzmann constant). From the graphical plotting of the experimental data  $\ln(\rho/T)$  vs.  $1/T$ , we have estimated the activation energy for the nanocrystalline and bulk counterparts by linear fitting using Eq. (1). The fitted results are shown in Figs. 2 and 3.

Regarding this context, it is important to mention that we have observed the remarkable modification of the activation energy due to the application of the external magnetic field and reduction of the particle size. The values of the activation energy are given in Table I for all the studied samples in different external magnetic fields in the paramagnetic region.

From the magneto-transport measurements and  $\rho(T)$  data analysis at the paramagnetic region, the summarized results are that (i) activation energy increases with the reduction of the particle size in the case of the nanocrystalline  $\text{La}_{0.46}\text{Ca}_{0.54}\text{MnO}_3$  compound and (ii) with the application of the 10 kOe magnetic field activation energy increases; however, it is reduced with the application of the 80 kOe magnetic field compared to the 0 kOe magnetic field. It is worth mentioning that the activation energy for the charge ordered nanoparticles (particle size  $\geq 45$  nm) is increased due to the application of the 10 kOe external magnetic field compared to the 0 kOe magnetic field. Such an increment may be associated with the training effect (transformation of meta-stable grain boundary spins to stable magnetic state), whereas in the presence of the 80 kOe magnetic field, the charge ordered fraction is destabilized and activation energy is reduced.

The correlation between the activation energy and crystallographic unit cell volume for doped manganite systems has been recently reported.<sup>24</sup> In our present study, the unit cell parameters were estimated from the room temperature XRD data (as mentioned earlier), and the unit cell volume was calculated for all the studied samples. The variation of the unit cell volume with particle size for the  $\text{La}_{0.46}\text{Ca}_{0.54}\text{MnO}_3$  compound is given in Fig. 4. Such an increasing nature of the unit cell volume with reduction of the particle size was also reported previously.<sup>23</sup>

Generally, in the case of the phase separated manganite systems, the external magnetic field reduces the activation energy resulting in negative magnetoresistance. In the case of the present study, activation energy increases due to the application of the 10 kOe external magnetic field at the paramagnetic region ( $T > 260$  K). In this context, magnetoresistance should also be different. We have calculated

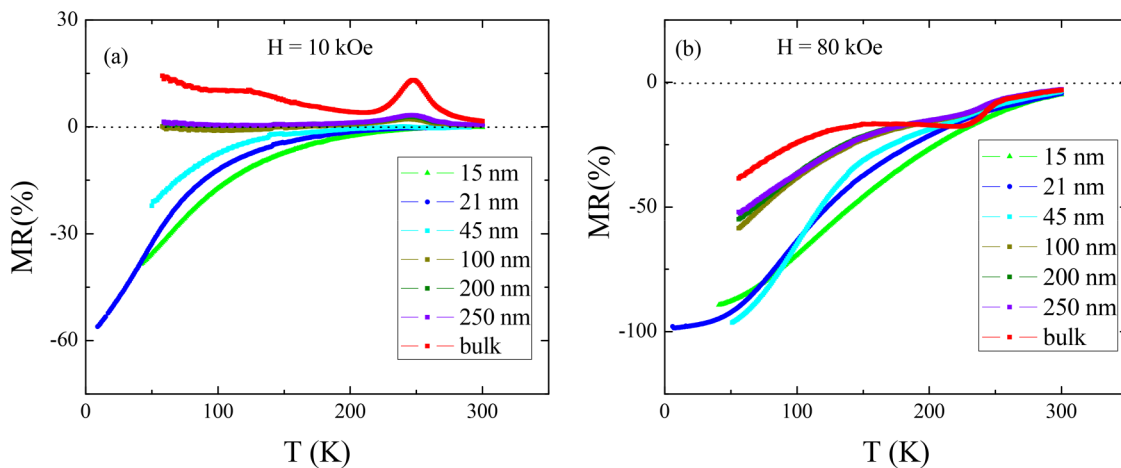


FIG. 5. Temperature dependent magnetoresistance for the  $\text{La}_{0.46}\text{Ca}_{0.54}\text{MnO}_3$  compound in the presence of 10 kOe and 80 kOe external magnetic field.

magnetoresistance for all studied compounds by using the equation given below

$$\text{MR}\% = \frac{R(H) - R(0)}{R(0)} \times 100. \quad (2)$$

Temperature dependent MR in the presence of external magnetic field 10 and 80 kOe is shown in Figs. 5(a) and 5(b), respectively. In context to the increase of activation energy in the presence of the 10 kOe magnetic field, we have observed small positive magnetoresistance which is shown in Fig. 5(a). The positive nature of the magnetoresistance is predominant in the case of the larger grain size samples (200 nm, 250 nm, and bulk counterparts). On the other hand, in the presence of 80 kOe external magnetic field, negative magnetoresistance is observed as usual [shown in Fig. 5(b)].

#### IV. CONCLUSIONS

To summarize, we have carried out the magneto-transport properties of charge ordered antiferromagnetic polycrystalline and the nanocrystalline  $\text{La}_{0.46}\text{Ca}_{0.54}\text{MnO}_3$  compound. Our experimental results indicate that the activation energy in the paramagnetic region is drastically influenced via the disorder and nucleation of the charge ordered domains in the different grain size samples. The correlation between the crystallographic unit cell and activation energy in the nanocrystalline compound has also been addressed (except for 15 and 21 nm particle size samples). For the 21 nm particle size sample, activation energy is much reduced compared to the 15 nm particle size sample due to the reduced disorder and spin-pinning effect. For the above mentioned two samples, systematic nature of the activation energy with magnetic field and particle size reduction is not observed due to the absence of the charge ordering in the lowest particle size sample. In addition to that, the anomalous magnetoresistance and increment of activation energy in the presence of lower values of the magnetic field (10 kOe) for the samples having particle sizes greater than 45 nm are explained by considering the training effect.

#### ACKNOWLEDGMENTS

This work was supported by the Department of Atomic Energy (DAE), Govt. of India. K.D. would like to acknowledge I. Das and Santanu Pakhira, Saha Institute of Nuclear Physics, for the experimental facilities and scientific discussions.

- <sup>1</sup>S. W. Cheong and H. Y. Hwang, *Contribution to Colossal Magnetoresistance Oxides*, Monographs in Condensed Matter Science, edited by Y. Tokura (Gordon and Breach, London, 1999).
- <sup>2</sup>*Colossal Magnetoresistive Oxides*, edited by Y. Tokura (Gordon and Breach Science, Amsterdam, 2000).
- <sup>3</sup>*Colossal Magnetoresistance, Charge Ordering and Related Properties of Manganese Oxides*, edited by C. N. R. Rao and R. Raveau (World Scientific, Singapore, 1998).
- <sup>4</sup>Y. Tokura, *Rep. Prog. Phys.* **69**, 797 (2006).
- <sup>5</sup>S. Dong, F. Gao, Z. Q. Wang, J. M. Liu, and Z. F. Ren, *Appl. Phys. Lett.* **90**, 082508 (2007).
- <sup>6</sup>S. Dong, R. Yu, S. Yunoki, J.-M. Liu, and E. Dagotto, *Phys. Rev. B* **78**, 064414 (2008).
- <sup>7</sup>Y. Tomioka, A. Asamitsu, H. Kuwahara, Y. Moritomo, and Y. Tokura, *Phys. Rev. B* **53**, R1689 (1996).
- <sup>8</sup>Y. Okimoto, Y. Tomioka, Y. Onose, Y. Otsuka, and Y. Tokura, *Phys. Rev. B* **57**, R9377 (1998).
- <sup>9</sup>K. Das, B. Satpati, and I. Das, *RSC Adv.* **5**, 27338 (2015).
- <sup>10</sup>K. Das, R. Rawat, B. Satpati, and I. Das, *Appl. Phys. Lett.* **103**, 202406 (2013).
- <sup>11</sup>S. Lee, H. Y. Hwang, B. I. Shraiman, W. D. Ratcliff, II, and S.-W. Cheong, *Phys. Rev. Lett.* **82**, 4508 (1999).
- <sup>12</sup>L. Pi, J. Cai, Q. Zhang, S. Tan, and Y. Zhang, *Phys. Rev. B* **71**, 134418 (2005).
- <sup>13</sup>K. R. Mavani and P. L. Paulose, *Europhys. Lett.* **78**, 37004 (2007).
- <sup>14</sup>N. S. Bingham, P. Lampen, M. H. Phan, T. D. Hoang, H. D. Chinh, C. L. Zhang, S. W. Cheong, and H. Srikanth, *Phys. Rev. B* **86**, 064420 (2012).
- <sup>15</sup>P. Lampen, A. Puri, M. H. Phan, and H. Srikanth, *J. Alloys Compd.* **512**, 94–99 (2012).
- <sup>16</sup>P. Lampen, N. S. Bingham, M. H. Phan, H. Kim, M. Osofsky, A. Pique, T. L. Phan, S. C. Yu, and H. Srikanth, *Appl. Phys. Lett.* **102**, 062414 (2013).
- <sup>17</sup>M. H. Phan, S. Chandra, N. S. Bingham, H. Srikanth, C. L. Zhang, S. W. Cheong, T. D. Hoang, and H. D. Chinh, *Appl. Phys. Lett.* **97**, 242506 (2010).
- <sup>18</sup>M. H. Phan and S. C. Yu, *J. Magn. Magn. Mater.* **308**, 325 (2007).
- <sup>19</sup>P. Lampen, N. S. Bingham, M. H. Phan, H. Srikanth, H. T. Yi, and S. W. Cheong, *Phys. Rev. B* **89**, 144414 (2014).
- <sup>20</sup>K. Das, P. Dasgupta, A. Poddar, and I. Das, *Sci. Rep.* **6**, 20351 (2016).
- <sup>21</sup>K. Das and I. Das, *J. Appl. Phys.* **118**, 084302 (2015).
- <sup>22</sup>H.-D. Zhou, G. Li, S.-J. Feng, Y. Liu, T. Qian, X.-J. Fan, and X.-G. Li, *Solid State Commun.* **122**, 507 (2002).
- <sup>23</sup>U. Shankar and A. K. Singh, *J. Phys. Chem. C* **119**, 28620 (2015).
- <sup>24</sup>H. S. Alagoz, I. Zivkovic, K. H. Chow, and J. Jung, *Phys. Chem. Chem. Phys.* **20**(4), 2431–2437 (2018).